

# Synthesis and electrochromic properties of aromatic polyimides bearing pendent triphenylamine units



Sheng-Huei Hsiao\*, Yu-Tan Chou

Department of Chemical Engineering and Biotechnology, National Taipei University of Technology, Taipei 10608, Taiwan, ROC

## ARTICLE INFO

### Article history:

Received 9 January 2014  
Received in revised form  
12 March 2014  
Accepted 19 March 2014  
Available online 25 March 2014

### Keywords:

Polyimides  
Triphenylamine  
Electrochromism

## ABSTRACT

A series of aromatic polyimides with pendent triphenylamine group were synthesized from equimolar mixtures of 4,4'-oxydianiline (ODA) and 4-(3,5-diaminobenzamido)triphenylamine (**4**), 4-(3,5-diaminobenzamido)-4',4''-di-*tert*-butyltriphenylamine (**t-Bu-4**) or 4-(3,5-diaminobenzamido)-4',4''-dimethoxytriphenylamine (**MeO-4**) with two aromatic tetracarboxylic dianhydrides (DSDA or 6FDA) via a conventional two-step procedure that included a ring-opening polyaddition to give poly(amic acid)s, followed by chemical imidization. These polyimides exhibited good solubility in polar organic solvents and could be solution-cast into flexible and strong films. They showed excellent thermal stability, with  $T_g$  values in the range of 284–309 °C. The polyimides derived from diamines **t-Bu-4** and **MeO-4** exhibited reversible electrochemical oxidation, accompanied by strong color changes with high contrast ratio and electrochromic stability. For the polyimides derived from diamine **4**, the coupling reaction between the triphenylamine radical cations occurred during the oxidative process forming a tetraphenylbenzidine structure, which resulted in an additional oxidation state and color change together with enhanced near-IR absorption at fully oxidized state.

© 2014 Elsevier Ltd. All rights reserved.

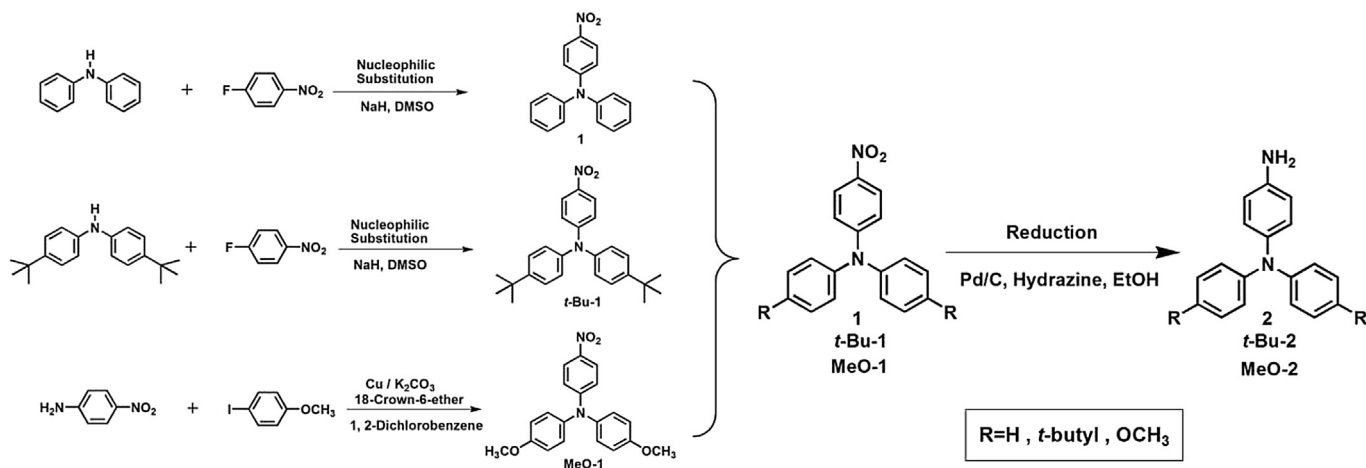
## 1. Introduction

Aromatic polyimides are commercially important materials used extensively in a wide range of optoelectronic applications due to their excellent chemical, thermal, and dielectric properties [1–4]. However, the technological applications of conventional polyimides are limited by processing difficulties because of high melting or glass-transition temperatures ( $T_g$ ) and limited solubility in most organic solvents due to their rigid backbones and strong interchain interactions. Thus, polyimide processing is generally carried out via the poly(amic acid) precursor, which is then converted to polyimide by vigorous thermal cyclodehydration. This process has inherent problems such as the emission of volatile by-products and storage instability of poly(amic acid) solution. To overcome these problems, many attempts have been made to synthesize soluble and processable polyimides in fully imidized form while maintaining their excellent properties [5–8]. One of the common methods used for increasing solubility and processability of polyimides without much sacrificing high thermal stability is the introduction of bulky, packing-disruptive groups into the polymer

backbone [9–20]. Incorporation of three-dimensional, propeller-shaped triphenylamine (TPA) unit into the polyimide backbone not only resulted in enhanced solubility [21–24] but also led to new electronic functionality of polyimides, such as electrochromic [25–30] and memory [31–36] characteristics, due to the redox-activity of the triarylamino core.

The anodic oxidation pathways of TPA have been extensively studied by Adams and co-workers [37]. The electrogenerated cation radical of TPA is not stable and could dimerize to form tetraphenylbenzidine by tail to tail coupling with the loss of two protons per dimer. When the phenyl groups were incorporated by bulky or electron-donating substituents such as *tert*-butyl and methoxy groups at the *para*-coupling sites of the TPA, the coupling reaction were greatly prevented [38–40]. It has been demonstrated that TPA-based polyimides generally exhibited poor electrochemical and electrochromic stability as compared to their polyamide analogs because of the strong electron-withdrawing imide group, which increases the oxidation potential of the TPA unit and destabilizes the resultant amino radical cation upon oxidation [41,42]. Attaching the TPA units as pendent groups on the polyimide backbone may improve the electrochemical and electrochromic stability of this kind of electroactive polymers. In this work, aromatic polyimides containing pendent TPA units were synthesized by incorporating the diamine components of **4**, **t-Bu-4** or **MeO-4**

\* Corresponding author. Tel.: +886 2 27712171x2548; fax: +886 2 27317117.  
E-mail address: [shhsiao@ntut.edu.tw](mailto:shhsiao@ntut.edu.tw) (S.-H. Hsiao).



Scheme 1. Synthesis of amino compounds **2**, **t-Bu-2**, and **MeO-2**.

into the polymer chain. The polyimides are expected to exhibit high thermal stability due to their aryl imide backbones, together with good solubility and redox-activity because of the laterally attached TPA groups. Furthermore, the incorporation of methoxy or *tert*-butyl substituents is expected to give extra electrochemical and electrochromic stability of the resulting polyimides.

## 2. Experimental

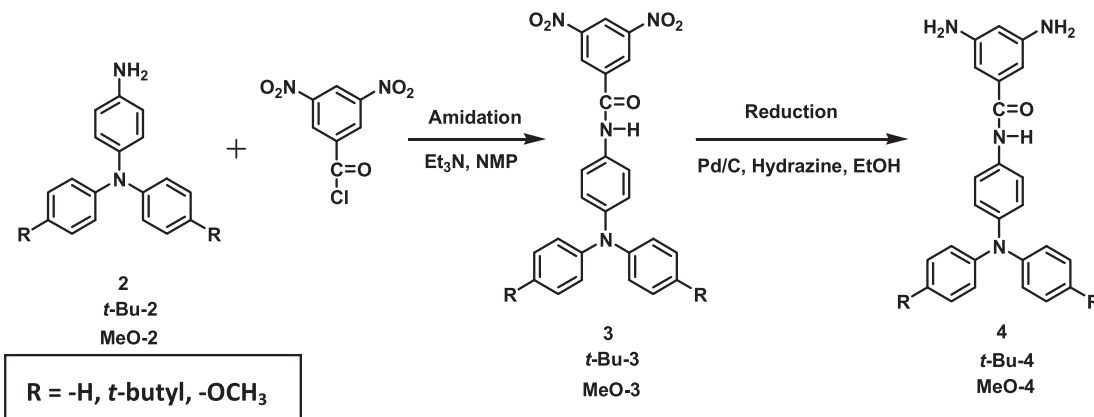
### 2.1. Materials

4-Aminotriphenylamine (**2**) (mp = 148–149 °C) [25] and 4-amino-4',4''-di-*tert*-butyltriphenylamine (**t-Bu-2**) (mp = 139–141 °C) [43] were synthesized by hydrazine Pd/C-catalyzed reduction of 4-nitrotriphenylamine (**1**) and 4,4'-di-*tert*-butyl-4''-nitrotriphenylamine (**t-Bu-1**) resulting from the fluoro-displacement reaction of *p*-fluoronitrobenzene with the sodium amide of aniline and bis(4-*tert*-butylphenyl)amine formed *in situ* by treatment with sodium hydride (Scheme 1). According to a reported method [44], 4-amino-4',4''-dimethoxytriphenylamine (**MeO-2**) (mp = 133–134 °C) was synthesized by hydrazine Pd/C-catalyzed reduction of 4-nitro-4',4''-dimethoxytriphenylamine (**MeO-1**) resulting from the Ullmann reaction of 4-nitroaniline with two equivalent amount of iodoanisole by using copper powder and potassium carbonate (K<sub>2</sub>CO<sub>3</sub>) in 1,2-dichlorobenzene. According to a known means [45–47], 4-(3,5-diaminobenzamido)triphenylamine (**4**), 4-(3,5-diaminobenzamido)-4',4''-di-*tert*-

butyltriphenylamine (**t-Bu-4**) and 4-(3,5-diaminobenzamido)-4',4''-dimethoxytriphenylamine (**MeO-4**) were prepared by the Pd/C-catalyzed hydrazine reduction of the corresponding dinitro compounds **3**, **t-Bu-3** and **MeO-3** obtained from the condensation of 3,5-dinitrobenzoyl chloride with amino compounds **2**, **t-Bu-2** and **MeO-2**, respectively, in *N*-methyl-2-pyrrolidone (NMP) in the presence of triethylamine (Scheme 2). Details of the synthetic procedures and characterization data of these diamine monomers are included in the Supporting Information (SI). *N,N*-Dimethylacetamide (DMAc, Fluka) was dried over calcium hydride for 24 h, distilled under reduced pressure, and stored over 4 Å molecular sieves in a sealed bottle. 3,3',4,4'-Diphenylsulfonetetracarboxylic dianhydride (DSDA; New Japan Chemical Co.) and 2,2-bis(3,4-dicarboxyphenyl)hexafluoropropane dianhydride (6FDA; Hoechst Celanese) were heated at 200 °C *in vacuo* for 3 h before use. Tetra-*n*-butylammonium perchlorate (Bu<sub>4</sub>NClO<sub>4</sub>) was obtained from Acros and recrystallized twice from ethyl acetate and then dried *in vacuo* before use. All other reagents were used as received from commercial sources.

### 2.2. Synthesis of polyimides

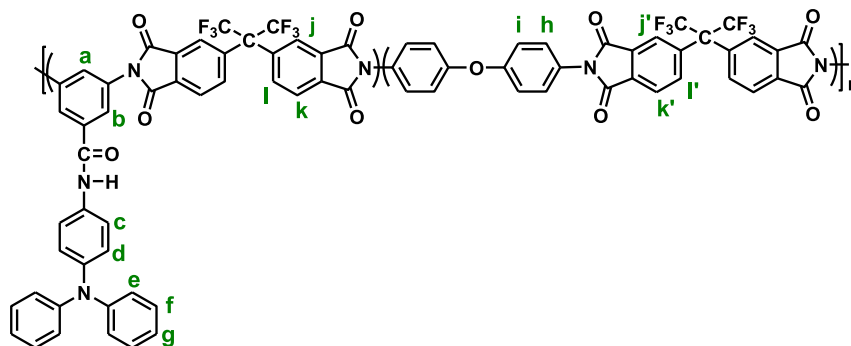
The polyimides were prepared from DSDA or 6FDA with an equimolar mixture of 4,4'-oxydianiline (ODA) and diamine **4**, **t-Bu-4**, or **MeO-4** by the conventional two-step method *via* chemical imidization reaction. A typical example for the preparation of polymer **5b** is given. A mixture of diamine **4** (0.1330 g, 0.25 mmol)



Scheme 2. Synthesis of diamine monomers **4**, **t-Bu-4**, and **MeO-4**.

and ODA (0.0675 g, 0.25 mmol) was dissolved in 4.8 mL of DMAc in a 50-mL round-bottom flask. Then dianhydride 6FDA (0.2995 g, 0.50 mmol) was added to the diamine solution in one portion. Thus, the solid content of the solution is approximately 10 wt %. The mixture was stirred at room temperature for about 3 h to yield a viscous poly(amic acid) solution. The inherent viscosity of the resulting poly(amic acid) was 1.10 dL/g, measured in DMAc at a concentration of 0.5 g/dL at 30 °C. Then, 2 mL of acetic anhydride and 1 mL of pyridine were added to the obtained poly(amic acid) solution, and the mixture was heated at 100 °C for 1 h to effect a complete imidization. The homogenous polymer solution was poured slowly into an excess of methanol giving rise to a pale yellow precipitate that was collected by filtration, washed thoroughly with hot water and methanol, and dried. The inherent viscosity of the resulting polyimide **5b** was 0.81 dL/g, measured in DMAc at a concentration of 0.5 g/dL at 30 °C. A polymer solution was made by the dissolution of about 0.4 g of the polyimide sample in 5 mL of hot DMAc. The homogeneous solution was poured into a 7-cm glass Petri dish, which was placed in a 90 °C oven overnight for the slow release of the solvent, and then the film was stripped off from the glass substrate and further dried in vacuum at 160 °C for 6 h.

The IR spectrum of **5b** (film) exhibited characteristic imide absorption bands at 1783  $\text{cm}^{-1}$  (asymmetrical C=O stretch), 1729  $\text{cm}^{-1}$  (symmetrical C=O stretch).  $^1\text{H}$  NMR (500 MHz,  $\text{DMSO}-d_6$ ,  $\delta$ , ppm): 6.97 (6H,  $\text{H}_e + \text{H}_g$ ), 7.01 (2H,  $\text{H}_d$ ), 7.23 (8H,  $\text{H}_i + \text{H}_f$ ), 7.48 (4H,  $\text{H}_h$ ), 7.67 (2H,  $\text{H}_c$ ), 7.75 (4H,  $\text{H}_j + \text{H}_k$ ), 7.80 (1H,  $\text{H}_a$ ), 7.96 (4H,  $\text{H}_l + \text{H}_l'$ ), 8.13 (1H,  $\text{H}_b$ ), 8.12 (4H,  $\text{H}_k + \text{H}_k'$ ), 10.41 (1H, amide proton).



### 2.3. Fabrication of electrochromic device

Electrochromic polymer film was prepared by dropping solution of the polyimide (4 mg/mL in DMAc) onto an ITO-coated glass substrate ( $20 \times 30 \times 0.7$  mm, 50–100  $\Omega/\text{square}$ ). The polymers were drop-coated onto an active area (about 20 mm  $\times$  20 mm) then dried in *vacuum*. A gel electrolyte based on PMMA (Mw: 120,000) and  $\text{LiClO}_4$  was plasticized with propylene carbonate to form a highly transparent and conductive gel. PMMA (1 g) was dissolved in dry acetonitrile (5 g), and  $\text{LiClO}_4$  (0.1 g) was added to the polymer solution as supporting electrolyte. Then, propylene carbonate (1.5 g) was added as plasticizer. The mixture was then slowly heated until gelation. The gel electrolyte was spread on the polymer-coated side of the electrode, and the electrodes were sandwiched. Finally, a transparent epoxy resin was used to seal the device.

### 2.4. Instrumentation and measurements

Infrared (IR) spectra were recorded on a Horiba FT-720 FT-IR spectrometer. Elemental analyses were run in a Heraeus VarioEL III

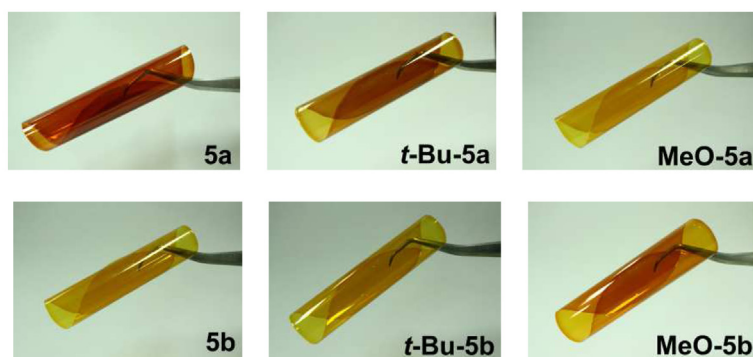
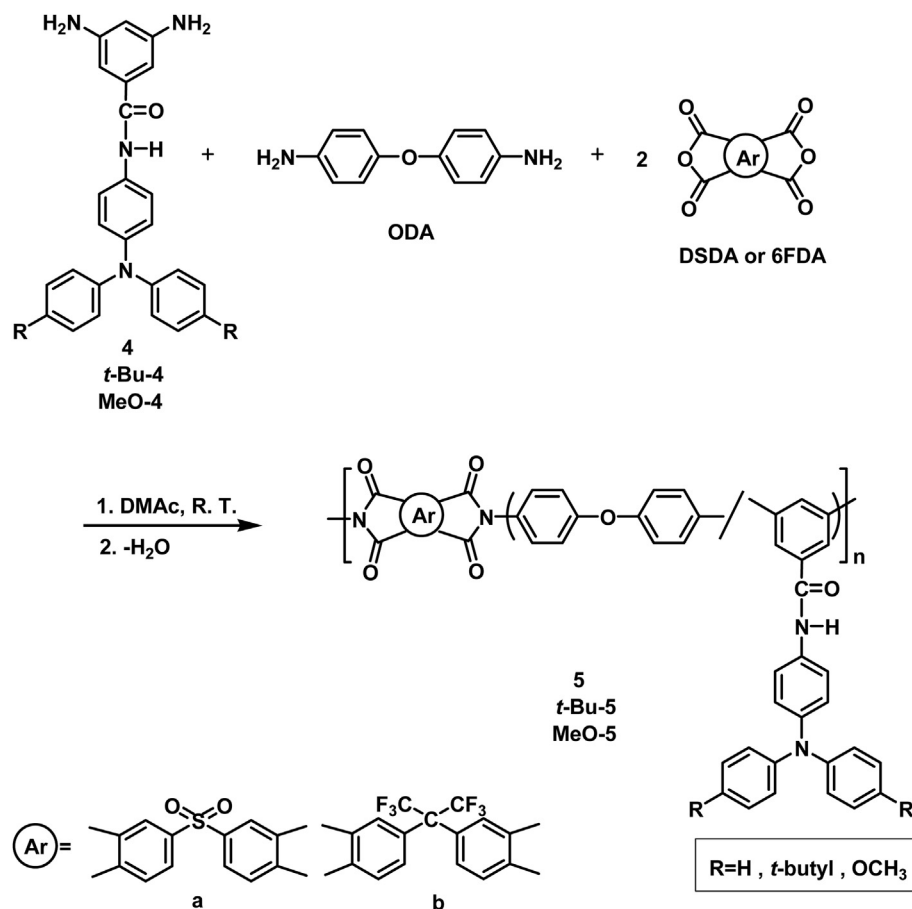
CHNS elemental analyzer.  $^1\text{H}$  and  $^{13}\text{C}$  NMR spectra were measured on a Bruker Avance 500 FT-NMR system. The chemical shifts in the NMR spectra were reported in parts per million (ppm) using tetramethylsilane as an internal standard. Splitting patterns were designed as s (singlet), d (doublet), t (triplet), or m (multiplet). The inherent viscosities were determined with a Cannon-Fenske viscometer at 30 °C. Wide-angle X-ray diffraction (WAXD) measurements were performed at room temperature (ca. 25 °C) on a Shimadzu XRD-6000 X-ray diffractometer with a graphite monochromator (operating at 40 kV and 30 mA), using nickel-filtered  $\text{Cu-K}\alpha$  radiation ( $\lambda = 1.5418 \text{ \AA}$ ). The scanning rate was  $2^\circ/\text{min}$  over a range of  $2\theta = 10\text{--}40^\circ$ . Thermogravimetric analysis (TGA) was performed with a Perkin–Elmer Pyris 1 TGA. Experiments were carried out on approximately 4–6 mg of samples heated in flowing nitrogen or air (flow rate = 40  $\text{cm}^3/\text{min}$ ) at a heating rate of 20 °C/min. DSC analyses were performed on a Perkin–Elmer Pyris 1 DSC at a scan rate of 20 °C/min in flowing nitrogen. Ultraviolet–visible (UV–Vis) spectra of the polymer films were recorded on an Agilent 8453 UV–Visible spectrometer. Cyclic voltammetry (CV) was performed with a CH Instruments 611C electrochemical analyzer using ITO as a working electrode (the coating area of the polymer film is approximately 1  $\text{cm}^2$ , 0.8 cm  $\times$  1.25 cm) and a platinum wire as an auxiliary electrode at a scan rate of 50 mV/s against a Ag/AgCl reference electrode in acetonitrile ( $\text{CH}_3\text{CN}$ ) or *N,N*-dimethylformamide (DMF) solution of 0.1 M  $\text{Bu}_4\text{NClO}_4$  under a nitrogen atmosphere. Spectroelectrochemistry analyses were carried out with an electrolytic cell, which was composed of a 1 cm cuvette, ITO

as a working electrode, a platinum wire as an auxiliary electrode, and a Ag/AgCl reference electrode. Absorption spectra in the spectroelectrochemical experiments were measured with an Agilent 8453 UV–Vis diode array spectrophotometer. Colorimetric measurements were obtained using a Minolta CS-100A Chroma Meter and the results are expressed in term of lightness ( $L^*$ ) and color coordinates ( $a^*$ ,  $b^*$ ). Coloration efficiency is derived from the equation:  $\eta = \Delta\text{OD}/Q_d$ ,  $\Delta\text{OD}$  is optical density change at specific absorption wavelength and  $Q_d$  is ejected charge determined from the *in situ* experiments.

## 3. Results and discussion

### 3.1. Polymer synthesis

Homopolymerization of any one of the diamine monomers **4**, **t-Bu-4**, and **MeO-4** with dianhydride DSDA or 6FDA just produced low-molecular-weight oligomers, which could not afford flexible films. Less favorable results from homopolymerization may be attributed to the formation of macrocyclic oligomers which limits ultimate molecular weights achievable during the polyaddition



**Scheme 3.** Synthesis of polyimides and images of their cast films.

**Table 1**  
Inherent viscosity and solubility behavior of polyimides.

Polymer code	$\eta_{inh}^a$ (dL/g)		Solubility in various solvents <sup>b</sup>					
	PAA	PI	NMP	DMAc	DMF	DMSO	<i>m</i> -cresol	THF
<b>5a</b>	0.89	0.66	++	++	++	++	+h	–
<b>5b</b>	1.10	0.81	++	++	++	++	+h	++
<b><i>t</i>-Bu-5a</b>	1.24	0.60	++	++	++	++	+h	++
<b><i>t</i>-Bu-5b</b>	1.19	0.88	++	++	++	++	+h	++
<b>MeO-5a</b>	1.17	0.62	++	++	++	++	+–	++
<b>MeO-5b</b>	1.21	0.86	++	++	++	++	+h	++

Notation: ++, soluble at room temperature; +h, soluble on heating at 100 °C; +–, partially soluble; –, insoluble even on heating. NMP: *N*-methyl-2-pyrrolidone; DMAc: *N,N*-dimethylacetamide; DMF: *N,N*-dimethylformamide; DMSO: dimethyl sulfoxide; THF: tetrahydrofuran.

<sup>a</sup> Inherent viscosity measured at a concentration of 0.5 g/dL in DMAc at 30 °C. PAA: poly(amic acid).

<sup>b</sup> Qualitative solubility was determined by using 10 mg sample in 1 mL of stirred solvent.

reactions of these meta-oriented phenylenediamines with the dianhydrides. In order to obtain polymers with sufficient molecular weights to permit the casting of tough films, we carried out the copolymerization of an equimolar mixture of ODA and each of the newly synthesized diamines with dianhydrides DSDA and 6FDA, respectively (Scheme 3). As shown in Table 1, the resulting poly(amic acid)s exhibited inherent viscosities of 0.89–1.24 dL/g. These poly(amic acid)s were chemically cyclodehydrated into the corresponding polyimides by treatment with a mixture of acetic anhydride and pyridine. The obtained polyimides were soluble in polar solvents such as DMAc. Therefore, the characterization of solution viscosity was carried out without any difficulty, and the inherent viscosities of these polyimides were recorded in the range of 0.60–0.88 dL/g, as measured in DMAc at 30 °C. All the polyimides could be solution cast to flexible and strong films (see the photos

shown in Scheme 1), indicating that they are high-molecular-weight polymers.

Structural features of these polyimides were characterized by IR and NMR analysis. A typical set of IR spectra of polyimide **5b** and its poly(amic acid) precursor are illustrated in SI Fig. S7. All polyimides exhibited characteristic imide group absorptions around 1780 and 1720  $\text{cm}^{-1}$  (typical of imide carbonyl asymmetrical and symmetrical stretch), 1380  $\text{cm}^{-1}$  (C–N stretch), and 1100 and 720  $\text{cm}^{-1}$  (imide ring deformation). Representative  $^1\text{H}$  NMR and H–H COSY NMR spectra of polyimide **MeO-5b** in  $\text{DMSO-}d_6$  are presented in Fig. 1. The NMR spectra of **5b** and **t-Bu-5b** are included in SI Figs. S8 and S9. All the aromatic protons resonated in the region of  $\delta$  6.8–8.2 ppm. The signals appearing around 10.3–10.4 ppm were

assigned to the pendent amide linkages. The signal appearing at 1.22 ppm in the  $^1\text{H}$  NMR spectrum of polyimide **t-Bu-5b** (Fig. S9) is peculiar to the *tert*-butyl groups, and that appearing at 3.70 ppm in the  $^1\text{H}$  NMR spectrum of polyimide **MeO-5b** (Fig. 1) is assigned to the methoxy substituents. Assignments of each proton are in good agreement with the structures of their repeating units.

### 3.2. Solubility of polyimides

The solubility of the polyimides in several organic solvents was investigated qualitatively, and the results are summarized in Table 1. All samples have been found soluble in aprotic polar solvents (NMP, DMAc, DMF, and DMSO) at room temperature. Except

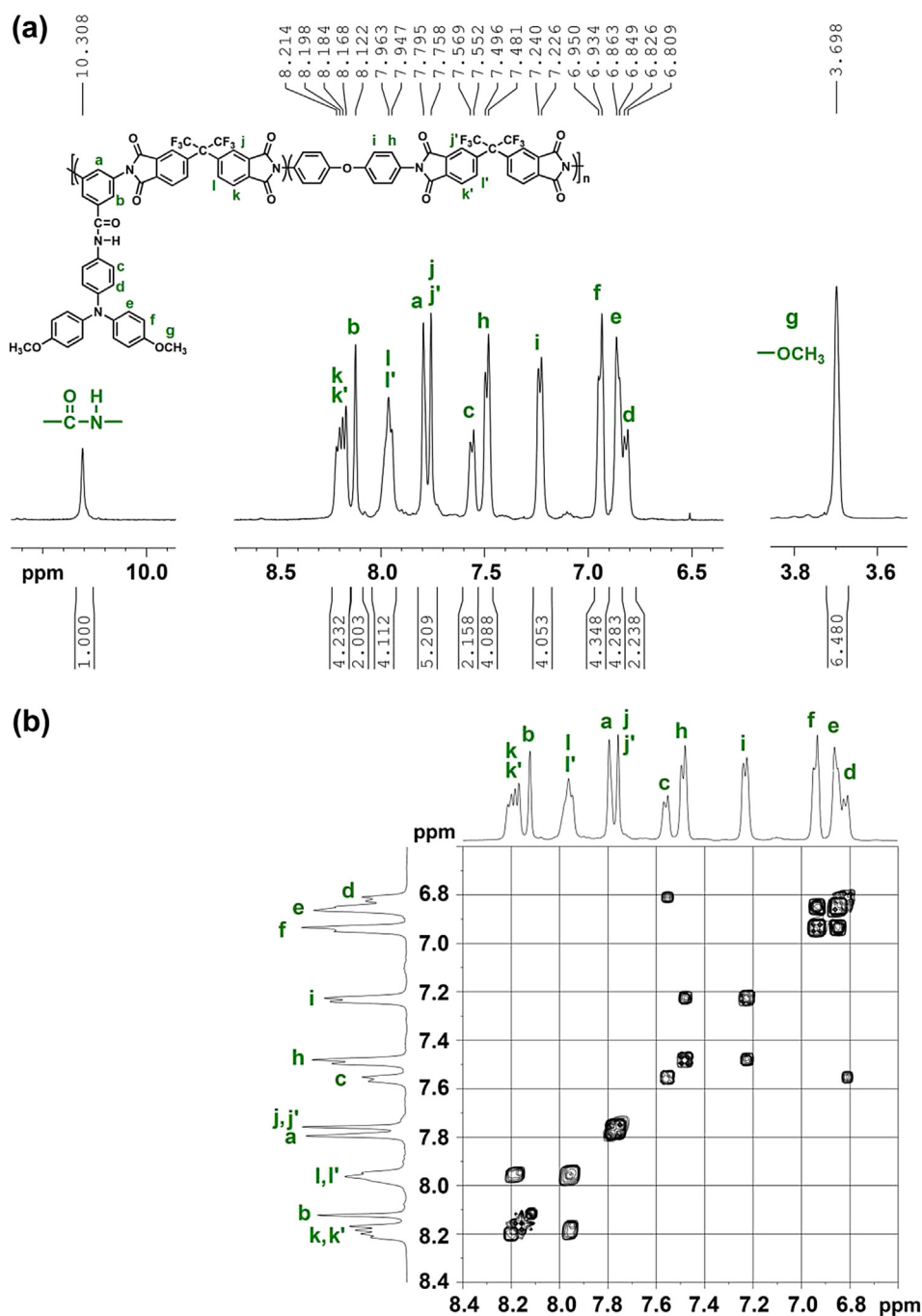


Fig. 1. (a)  $^1\text{H}$  NMR spectrum and (b) H–H COSY spectrum of polyimide **MeO-5b**.

for polyimide **5a**, all of them are also readily soluble in THF. The high solubility can be attributed in part to the introduction of the bulky pendent TPA moiety into the repeat unit. The excellent solubility makes these polymers potential candidates for practical applications by common solution processes to afford high performance thin films for optoelectronic devices. As shown in Fig. S10 (SI), all the polyimides showed amorphous WAXD patterns. This result is reasonable because the bulky pendent groups and random repeat units do not favor their close chain packing.

### 3.3. Thermal properties

The thermal stability and phase-transition temperatures of these polyimides were investigated by TGA, DSC, and TMA techniques. The thermal behavior data are summarized in Table 2. DSC measurements were conducted with a heating rate of 20 °C/min in nitrogen. Quenching from an elevated temperature of about 400 °C to 50 °C gave predominantly amorphous samples so that the glass transition temperatures ( $T_g$ ) of all the polyimides could be easily determined in the second heating traces of DSC (Fig. S11, SI).  $T_g$  values of these polyimides were recorded in the range 284–309 °C. Higher  $T_g$  values for the polyimides **t-Bu-5a** and **t-Bu-5b** as compared with the other counterparts can be attributed to the bulky *tert*-butyl groups thus restricting the segment mobility. The softening temperatures ( $T_s$ ) (may be referred to as apparent  $T_g$ ) of the polymer film samples were determined by TMA method with a loaded penetration probe. These polyimides exhibited  $T_s$  values of 284–295 °C.

Fig. S12 compares the TGA thermograms of **5a**, **t-Bu-5a** and **MeO-5a** in both air and nitrogen atmospheres. All the prepared polyimides exhibited good thermal stability with no significant weight loss up to 450 °C in nitrogen or air atmosphere. Decomposition temperatures ( $T_d$ ) at a 10% weight loss of these polymers in nitrogen and air were recorded in the range of 469–552 and 486–552 °C, respectively. The amount of carbonized residue (char yield) of these polymers in nitrogen atmosphere was more than 45% at 800 °C. Polyimides **t-Bu-5** and **MeO-5** series exhibited a lower  $T_d$  value as compared with the corresponding **5** ones without substituents on the pendent phenyl rings. This is reasonable when considering the less stable aliphatic segments. The DSDA polyimides showed a relatively lower  $T_d$  and char yield as compared to the 6FDA polyimides due to the less stable sulfonyl group.

**Table 2**  
Thermal properties of the polyimides.

Polymer <sup>a</sup> code	$T_g$ (°C) <sup>b</sup>	$T_s$ (°C) <sup>c</sup>	$T_d$ at 10% weight loss (°C) <sup>d</sup>		Char yield (wt %) <sup>e</sup>
			In N <sub>2</sub>	In air	
<b>5a</b>	302	293	510	543	48
<b>5b</b>	296	284	552	552	54
<b>t-Bu-5a</b>	309	300	490	486	45
<b>t-Bu-5b</b>	298	291	542	530	54
<b>MeO-5a</b>	284	289	469	493	48
<b>MeO-5b</b>	287	295	531	531	53

<sup>a</sup> All the polymer films were heated at 300 °C for 1 h prior to DSC, TMA and TGA experiments.

<sup>b</sup> Midpoint temperature of the baseline shift on the second DSC heating trace (rate = 20 °C/min) of the sample after quenching from 400 to 50 °C (cooling rate = 200 °C/min) in nitrogen.

<sup>c</sup> Softening temperature measured by TMA with a constant applied load of 10 mN at a heating rate of 10 °C/min.

<sup>d</sup> Decomposition temperature at which a 10% weight loss was recorded by TGA at a heating rate of 20 °C/min.

<sup>e</sup> Residual weight % at 800 °C at a scan rate 20 °C/min in nitrogen.

### 3.4. Electrochemical properties

The anodic and cathodic electrochemical properties of the cast polyimide films on the ITO electrodes were assessed by cyclic voltammetry (CV) using a conventional three-electrode cell assembly. The oxidation and reduction cycles of the film samples were measured in acetonitrile and DMF, respectively, using Bu<sub>4</sub>NClO<sub>4</sub> as the electrolyte. All the polyimides showed a reversible oxidation process in their first CV scans at around 0.66–0.97 V ( $E_{1/2}^{ox}$ ) that corresponds to the TPA oxidation. Typical CV curves of polyimides **5a**, **t-Bu-5a**, and **MeO-5a** are shown in Fig. 2. As expected, polyamide **MeO-5a** exhibited a lower oxidation potential ( $E_{onset} = 0.58$  V) than **t-Bu-5a** ( $E_{onset} = 0.69$  V) and **6b** ( $E_{onset} = 0.88$  V) because of the electron-donating methoxy substituents on the pendent phenyl rings of the TPA unit.

The repetitive CV scanning results for polyimide **5a** are shown in Fig. S13. Upon repetitive scanning for polyimide **5a** over the voltage range from 0 to 1.20 V, a new oxidation wave appeared as a shoulder at 0.86 V since the second scan. This is a typical oxidation wave of the benzidine group, indicating the occurrence of the oxidative coupling between the TPA units. As suggested in Fig. S14, the TPA radical cations may dimerize to a tetraphenylbenzidine (TPB) segment that is easier to oxidize than the parent TPA unit. The electrochemical properties of the analogous polyimide **MeO-5a** are completely different. Repetitive scans between 0 and 0.90 V at a scan rate of 50 mV/s provided the same patterns as that observed in the first scan. The curves were affected by only the diffusion contribution, and no new waves were detected under these experimental conditions. This reversible oxidation process suggests that the radical cations of **MeO-5a** are more stable than those produced from the oxidation of **5a**. The *tert*-butyl-substituted analogs showed a similar

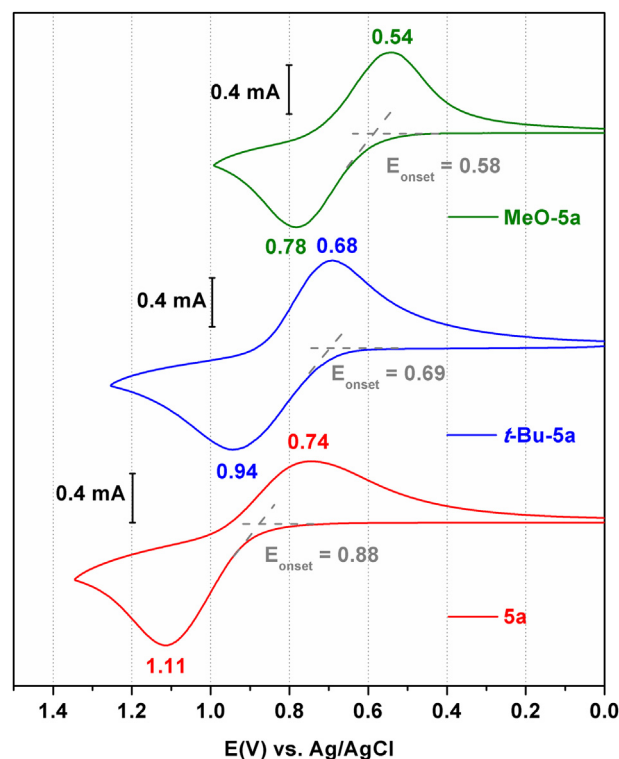


**Fig. 2.** Anodic cyclic voltammograms of the cast films of polyimides **5a**, **t-Bu-5a**, and **MeO-5a** on an ITO-coated glass substrate in 0.1 M Bu<sub>4</sub>NClO<sub>4</sub>/CH<sub>3</sub>CN solution at a scan rate of 50 mV/s.

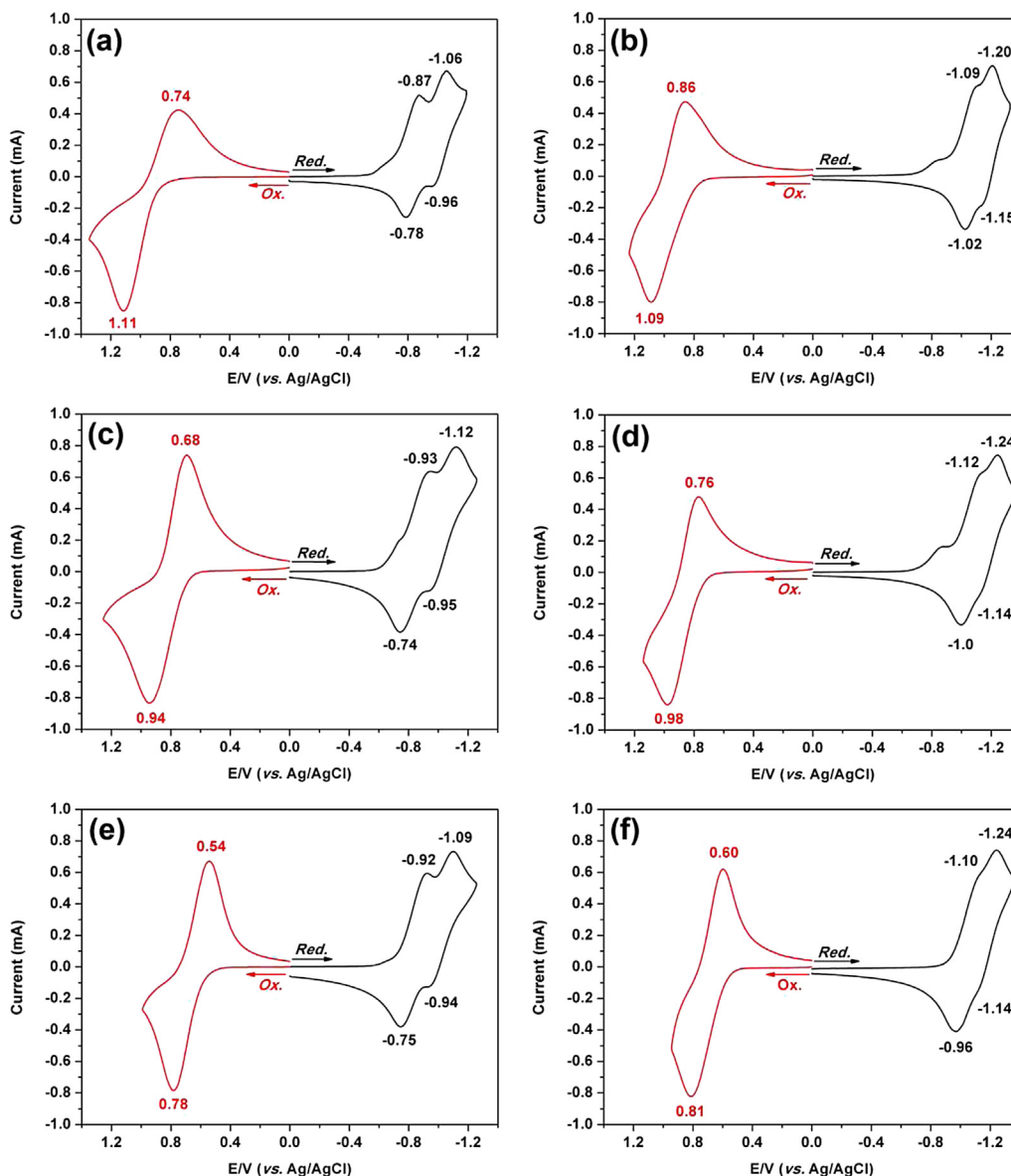


**Fig. 3.** Cyclic voltammograms of the cast films of polyimides (a) **5a**, (b) **5b**, (c) **t-Bu-5a**, (d) **t-Bu-5b**, (e) **MeO-5a**, and (f) **MeO-5b** on an ITO-coated glass substrate in 0.1 M Bu<sub>4</sub>NClO<sub>4</sub>/CH<sub>3</sub>CN (for anodic process) and DMF (for cathodic process) solution at a scan rate of 50 and 100 mV/s, respectively.

electrochemical behavior as that of **MeO-5a**. Thus, incorporation of bulky *tert*-butyl or electron-donating methoxy groups on the active sites of the TPA unit greatly prevents the coupling reaction of these electroactive polyimides. As illustrated in Fig. 3, all the polyimides exhibited additional two quasi-reversible reduction

peaks at  $E_{pc} = -0.87 \sim -1.12$  V and  $-1.06 \sim -1.24$  V due to the electron-charging on the phthalimide units. Due to the strong electron-withdrawing property of the sulfonyl group, the imide segment derived from DSDA can be reduced at a less negative potential.

**Table 3**

Redox potentials and energy levels of polyimides.

Polymer code	Thin film (nm)		Oxidation potential (V) <sup>a</sup>		Reduction potential (V) <sup>b</sup>			$E_g^{\text{opt}}$ (eV) <sup>c</sup>	HOMO (eV) <sup>d</sup>	LUMO (eV) <sup>d</sup>
	$\lambda_{\text{max}}^{\text{abs}}$	$\lambda_{\text{onset}}^{\text{abs}}$	$E_{\text{onset}}^{\text{ox}}$	$E_{1/2}^{\text{ox}}$	$E_{\text{onset}}^{\text{red}}$	$E_{1/2}^{\text{red1}}$	$E_{1/2}^{\text{red2}}$			
<b>5a</b>	301	397	0.88	0.92	-0.68	-0.82	-1.01	3.18	5.28	2.10
<b>5b</b>	297	397	0.79	0.97	-0.91	-1.05	-1.17	3.12	5.33	2.21
<b>t-Bu-5a</b>	304	402	0.69	0.81	-0.70	-0.83	-1.03	3.05	5.17	2.12
<b>t-Bu-5b</b>	300	407	0.72	0.87	-0.90	-1.06	-1.19	3.05	5.23	2.18
<b>MeO-5a</b>	297	408	0.58	0.66	-0.71	-0.84	-1.01	2.94	5.02	2.08
<b>MeO-5b</b>	295	409	0.57	0.70	-0.94	-1.03	-1.19	2.90	5.06	2.16

<sup>a</sup> vs. Ag/AgCl in CH<sub>3</sub>CN.

<sup>b</sup> vs. Ag/AgCl in DMF.  $E_{1/2}$ : the half-wave potential (Average potential of the redox couple peaks).

<sup>c</sup> The data were calculated from polymer films by the equation:  $E_g^{\text{opt}} = 1240/\lambda_{\text{onset}}$ .

<sup>d</sup> The HOMO and LUMO energy levels were calculated from  $E_{\text{onset}}^{\text{ox}}$  values of CV curves and were referenced to ferrocene (4.8 eV relative to the vacuum energy level).

The energy levels of the highest occupied molecular orbital (HOMO) and lowest unoccupied molecular orbital (LUMO) of the corresponding polymers were estimated from the  $E_{1/2}^{OX}$  values. Assuming that the HOMO energy level for the ferrocene/ferrocenium ( $Fe/Fe^+$ ) standard is 4.8 eV with respect to the zero vacuum level, the HOMO and LUMO values for these polyimides were calculated to be in the range of 5.02–5.33 eV and 2.08–2.21 eV, respectively. The redox potentials and energy levels of all the polyimides are summarized in Table 3.

### 3.5. Spectroelectrochemical and electrochromic properties

The electro-optical properties of the polymer films were investigated using the changes in electronic absorption spectra at various applied voltages. For these investigations, the polyimide film was cast on an ITO-coated glass slide (a piece that fit in the UV–vis cuvette), and a homemade electrochemical cell was built from a commercial UV–vis cuvette. The cell was placed in the optical path of the sample light beam in a commercial diode array spectrophotometer. This procedure allowed us to obtain electronic absorption spectra under potential control in a 0.1 M  $Bu_4NClO_4$ /acetonitrile or DMF solution. The result of the **5b** film upon electro-oxidation is presented in Fig. 4a as a series of UV–vis–NIR absorption curves correlated to electrode potentials. In the neutral form, at 0.0 V, polyimide **5b** exhibited strong absorption at wavelength around 301 nm, characteristic for TPA, but it is almost transparent in the visible region ( $L^*$ : 91;  $a^*$ : 2;  $b^*$ : 1). As the applied voltage was stepped from 0 to 0.8 V, the intensity of the absorption peak at 301 nm decreased slightly and new peaks at 400, 500 and 750 nm gradually increased in intensity. In the same time, the film turned into a greenish-blue color. We attribute these spectral changes to the formation of a stable cation radical of the side-chain

TPA moiety. Further increase of the applied voltage to 1.1 V led to an additional strong absorption in the near-IR region (around 875 nm) with the color changed to blue ( $L^*$ : 55;  $a^*$ : –6;  $b^*$ : –24). This result may be caused by the oxidation of the TPB moiety formed *in situ* during the potential scan. After the first electrochemical series of polyimide **5b** was recorded from 0 to 1.1 V and then back to 0 V, we re-applied the electrode voltage. As shown in Fig. 4b, when the applied voltage was stepped from 0 to 0.8 V, in addition to a small band at 750 nm, a new small absorption at 490 nm emerged. Meanwhile, the film changed from colorless to orange ( $L^*$ : 70;  $a^*$ : 3;  $b^*$ : 15). The new orange oxidized state may be attributed to the first oxidation of the TPB unit resulted from the coupling reaction occurred on the active sites of the side-chain TPA unit (Fig. S14). When the applied voltage was stepped to 1.1 V, the spectral and color changes of the film are similar to those observed in the first spectroelectrochemical series. These results indicated that the occurrence of the second step oxidation of the TPB moieties associated with the oxidation of the residual TPA units. A similar spectral change was also observed for polyimide **5a**.

Spectral changes of polyimide **MeO-5b** at various applied potentials are illustrated in Fig. 4c. When the applied potential was gradually increased from 0 to 0.8 V, the electrochromic film of **MeO-5b** showed new absorptions at around 380 and 750 nm with increasing intensity. As shown in Fig. 4d, the spectral changes of the second spectroelectrochemical series are very similar to those in the first series. For polyimide **t-Bu-5b**, its film revealed a medium absorption at 388 nm and a strong absorption band centered at 750 nm at an applied potential of 1.0 V (Fig. 5a). Both of these two polymer films were associated with significant color change from colorless ( $L^*$ : 96;  $a^*$ : 1;  $b^*$ : 2) to cyan ( $L^*$ : 61;  $a^*$ : –2;  $b^*$ : –8) or blue ( $L^*$ : 30;  $a^*$ : –3;  $b^*$ : –29) upon electro-oxidation. No remarkable absorptions at 490 nm and in the near-IR region were observed

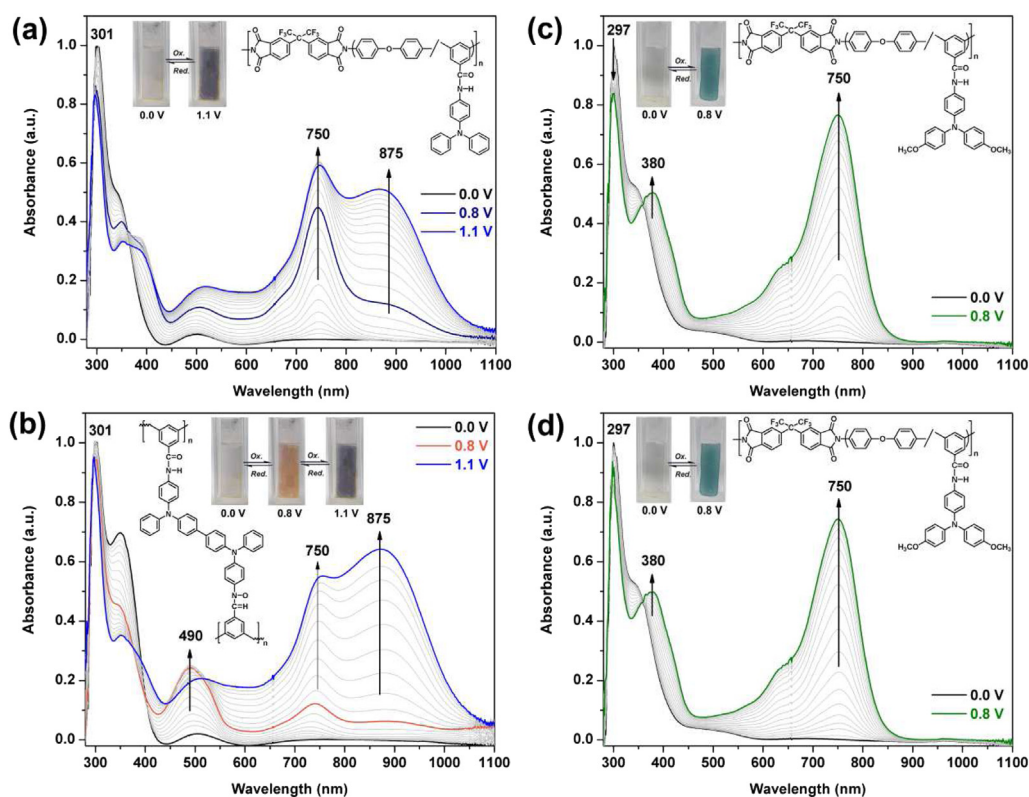
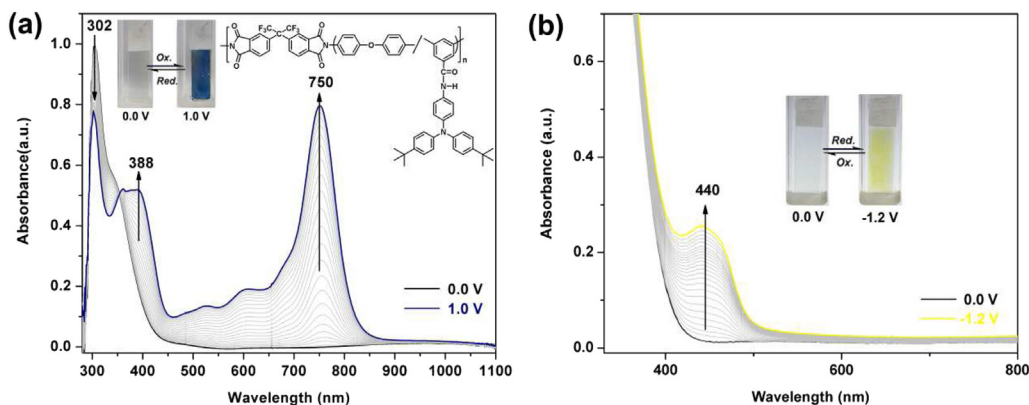


Fig. 4. Spectral changes of the cast film of polyimides on an ITO-coated glass in 0.1 M  $Bu_4NClO_4/CH_3CN$  at various applied potentials (vs.  $Ag/AgCl$ ): (a) the first series for polyimide **5b**, (b) the second series for polyimide **5b**, (c) the first series for polyimide **MeO-5b**, and (d) the second series for polyimide **MeO-5b**.



**Fig. 5.** Spectroelectrochemistry of polyimide **t-Bu-5b** thin film on the ITO-coated glass substrate in 0.1 M  $\text{Bu}_4\text{NClO}_4/\text{CH}_3\text{CN}$  (for the anodic oxidation) or DMF (for the cathodic reduction) at various applied potentials.

during the oxidation process of these two polyimides. This result illustrated that almost no benzidine moieties was produced during the oxidation process. Fig. 5b illustrates the spectral and coloration changes of **t-Bu-5b** on electro-reduction. However, the color change from colorless to light yellow ( $L^*$ : 81;  $a^*$ : 1;  $b^*$ : 5) is not strong as that observed in the anodic scanning.

### 3.6. Electrochromic switching and stability

Electrochemical switching studies for the polyimides were performed to monitor the percent transmittance change ( $\Delta\%T$ ) as a function of time at their absorption maximum ( $\lambda_{\text{max}}$ ) and to determine the response time by stepping potential repeatedly between the neutral and oxidized states. The active area of the polymer film on ITO glass is about  $1 \text{ cm}^2$ . Fig. 6 depicts the optical transmittance change of polyimides **5b**, **t-Bu-5b**, and **MeO-5b** as a function of time at 750 nm by applying square-wave potential steps of 10 s (complete cycle time is 20 s) between 0 and 1.1, 1.0, and 0.8 V, respectively. The switching time was defined as the time that was required to reach 90% of the full change in absorbance after switching potential because it is difficult to perceive any further color change with naked eye beyond this point. The optical contrast measured as  $\Delta\%T$  of these polymers between neutral and oxidized blue states was found to be 72% for **5b**, 85% for **t-Bu-5b**, and 83% for **MeO-5b**, respectively. The electrochromic properties of the polyimide films during n-doping processes are summarized in Table 4.

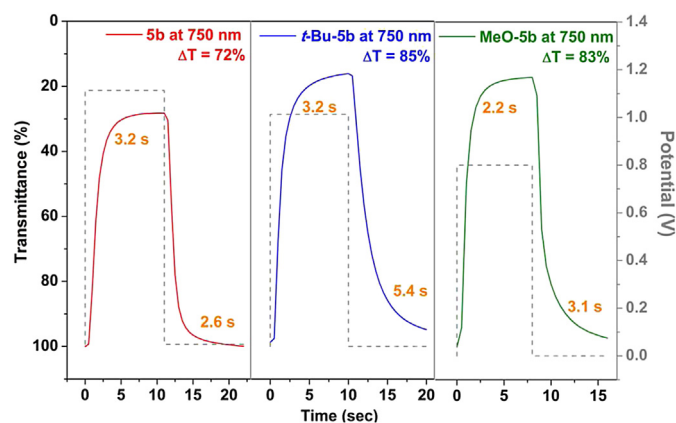


**Fig. 6.** Optical transmittance change monitored at 750 nm for the polyimide thin films ( $\sim 150 \text{ nm}$  in thickness) on ITO-glass slide in 0.1 M  $\text{Bu}_4\text{NClO}_4/\text{CH}_3\text{CN}$ . (The dotted line represents the applied voltage.)

The coloration efficiencies of these three polyimides were calculated to be in the range of  $211\text{--}320 \text{ cm}^2/\text{C}$ .

The switching stability of the polyimides was investigated by monitoring the electrochromic contrast ( $\Delta\%T$ ) of the thin films on repeated square-wave potential steps between their neutral and oxidized states. Fig. 7a–c shows the results of first ten cycles of polyimides **5b**, **t-Bu-5b**, and **MeO-5b**, respectively. Polyimides **t-Bu-5b** and **MeO-5b** exhibited better reversibility of electrochromic characteristics than **5b** in the first ten cycles. Therefore, the introduction of the *para*-substituted methoxy or *tert*-butyl groups on the pendent diphenylamino unit effectively prevent the tail to tail coupling reaction and could increase the electrochromic stability of these polyimides. After 50 cycles polyimide **MeO-5b** still preserved good electrochromic reversibility and moderate optical contrast (Fig. 7d).

### 3.7. Electrochromic device

Based on the foregoing results, it can be concluded that these polyimides can be used in the construction of electrochromic devices and optical display due to the fast response time and the robustness of the polymers. Therefore, we fabricated as preliminary investigations single layer electrochromic cells (Fig. 8). The polyimide films were cast onto the ITO-coated glass and then dried. Afterward, the gel electrolyte was spread on the polymer-coated side of the electrode and the electrodes were sandwiched. To prevent leakage, an epoxy resin was applied to seal the device. As a typical example, an electrochromic cell based on polyimide **MeO-5b** was fabricated. The polymer film is colorless or very pale yellow in the neutral form. When the applied voltage was increased to 1.8 V, the film changed to cyan in color due to electro-oxidation. When the potential was subsequently set back at 0 V, the

**Table 4**  
Electrochromic properties of polyimides.

Polymer code	$\lambda_{\text{max}}$ (nm)	Voltage (V)	$\Delta\%T$	Response time <sup>a</sup>		$\Delta\text{OD}^b$	$Q_d^c$ (mC/cm <sup>2</sup> )	CE <sup>d</sup> (cm <sup>2</sup> /C)
				$t_c$ (s)	$t_b$ (s)			
<b>5b</b>	750	1.1	72	3.2	2.6	0.41	1.94	211
<b>t-Bu-5b</b>	750	1.0	85	3.2	5.4	0.55	1.84	298
<b>MeO-5b</b>	750	0.8	83	2.2	3.1	0.54	1.73	320

<sup>a</sup> Time for 90% of the full-transmittance change.

<sup>b</sup> Optical density ( $\Delta\text{OD}^b$ ) =  $\log[T_{\text{bleached}}/T_{\text{colored}}]$ , where  $T_{\text{colored}}$  and  $T_{\text{bleached}}$  are the maximum transmittance in the oxidized and neutral states, respectively.

<sup>c</sup>  $Q_d$  is ejected charge, determined from the *in situ* experiments.

<sup>d</sup> Coloration efficiency (CE) =  $\Delta\text{OD}/Q_d$ .

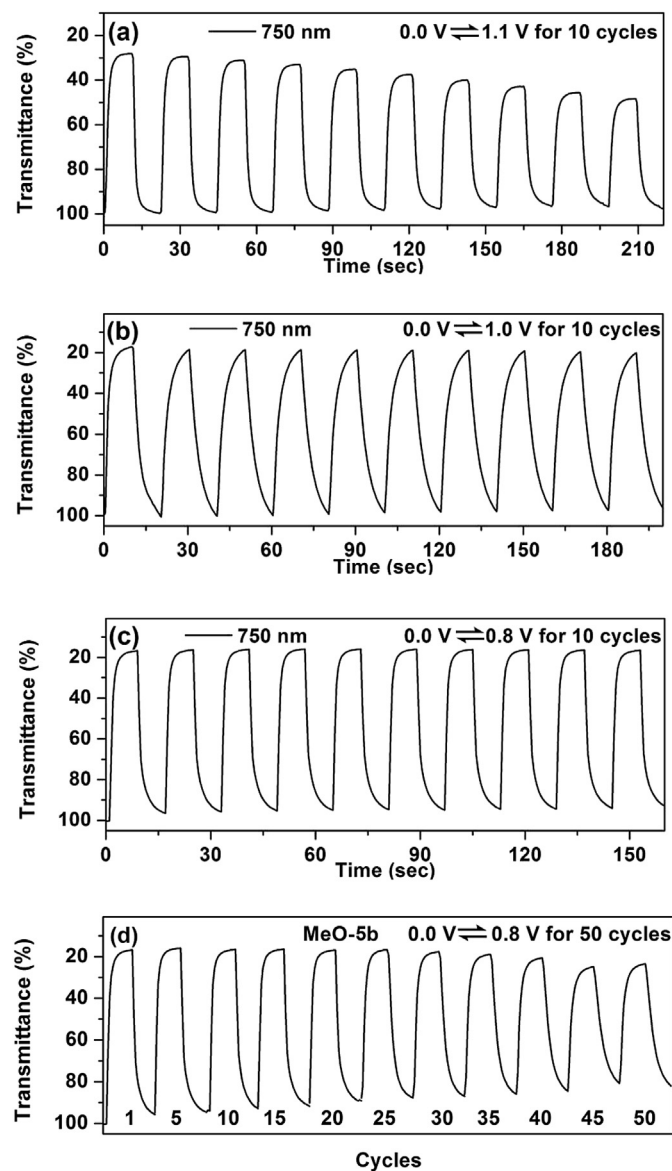


Fig. 7. Potential step absorptometry of the cast films (~150 nm in thickness) of polyimides on the ITO-glass slide by applying a potential step: (a) **5b** (b) **t-Bu-5b** (c) **MeO-5b** for 10 cycles and (d) **MeO-5b** for 50 cycles.

polymer film turned back to original pale yellow. We believe that optimization could further improve the device performance and fully explore the potential of these electrochromic polyimides.

#### 4. Conclusions

A new series of electroactive polyimides incorporated with pendent triphenylamine group as a redox-chromophore have been synthesized. All the polyimides could form morphologically stable and uniform amorphous films by the solution-casting technique. In addition to high  $T_g$  and high thermal stability, the polyimides also revealed ambipolar electrochemical and electrochromic characteristics. Incorporating bulky *tert*-butyl or electron-donating methoxy substituents at the *para*-positions of pendent diphenylamino group not only stabilizes the TPA radical cations but also leads to lower oxidation potentials of the polyimides. For the polyimides derived from the diamine **4** (without substituents on its TPA unit), the TPA radical cations formed during the oxidative process could

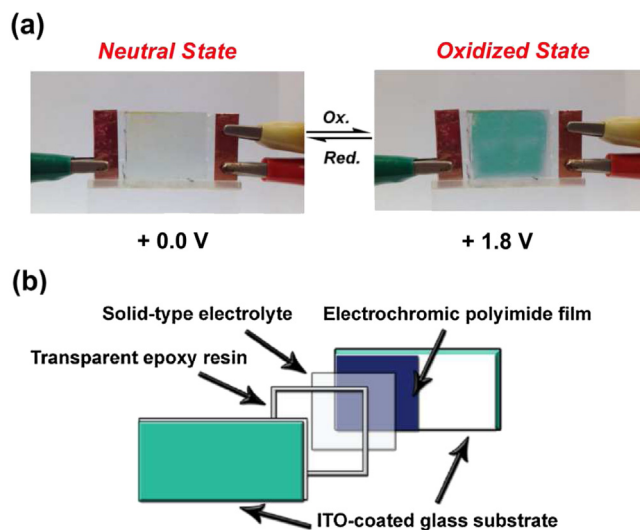


Fig. 8. (a) Photos of single-layer ITO-coated glass electrochromic device, using polyimide **MeO-5b** as active layer. (b) Schematic diagram of polyimide ECD sandwich cell.

dimerize to a benzidine structure which led to additional oxidation states and color change together with a strong near-IR absorption at their fully oxidized states. Thus, these characteristics suggest that this new class of polyimides has great potential for use in optoelectronics applications such as electrochromic devices.

#### Acknowledgment

We thank the financial support from the National Science Council in Taiwan, ROC.

#### Appendix A. Supplementary data

Supplementary data related to this article can be found at <http://dx.doi.org/10.1016/j.polymer.2014.03.031>.

#### References

- [1] Wilson D, Stenzenberger HD, Hergenrother PM. Polyimides. Glasgow and London: Blackie; 1990.
- [2] Sroog CE. Prog Polym Sci 1991;16:561–694.
- [3] Ghosh MK, Mittal KL. Polyimides: fundamentals and applications. New York: Marcel Dekker; 1996.
- [4] Liaw DJ, Wang KL, Huang YC, Lee KR, Lai JY, Ha CS. Prog Polym Sci 2012;37:907–74.
- [5] Huang SJ, Hoyt AE. Trends Polym Sci 1995;3:262–71.
- [6] de Abajo J, de la Campa JG. Adv Polym Sci 1999;140:23–59.
- [7] Ding M. Prog Polym Sci 2007;32:623–68.
- [8] Dhara MG, Banerjee S. Prog Polym Sci 2010;35:1022–77.
- [9] Yin DX, Li YF, Yang HX, Yang SY, Fan L, Liu JG. Polymer 2005;46:3119–27.
- [10] Kim YH, Kim HS, Kwon SK. Macromolecules 2005;38:7950–6.
- [11] Zhang QY, Chen G, Zhang SB. Polymer 2007;48:2250–6.
- [12] Zhang QY, Li SH, Li WM, Zhang SB. Polymer 2007;48:6246–53.
- [13] Chern YT, Tsai JY. Macromolecules 2008;41:9556–64.
- [14] Chern YT, Tsai JY, Wang JJ. J Polym Sci Part A: Polym Chem 2009;47:2443–52.
- [15] Zhang SJ, Li YF, Ma T, Zhao JJ, Xu XY, Yang FC, et al. Polym Chem 2010;1:485–93.
- [16] Lin CH, Chang SL, Peng IA, Peng SP, Chung YH. Polymer 2010;51:3899–906.
- [17] Lin CH, Chang SL, Cheng PW. J Polym Sci Part A: Polym Chem 2011;49:1331–40.
- [18] Hsiao SH, Wang HM, Chen WJ, Lee TM, Leu CM. J Polym Sci Part A: Polym Chem 2011;49:3109–20.
- [19] Hsiao SH, Wang HM, Chou JS, Guo WJ, Lee TM, Leu CM, et al. J Polym Res 2012;19:9757 (12 pages).
- [20] Kim SD, Lee S, Heo J, Kim SY, Chung IS. Polymer 2013;54:5648–54.
- [21] Oishi Y, Ishida M, Kakimoto M, Imai Y, Kurosaki T. J Polym Sci Part A: Polym Chem 1992;30:1027–35.
- [22] Liou GS, Hsiao SH, Ishida M, Kakimoto M, Imai Y. J Polym Sci Part A: Polym Chem 2002;40:3815–22.

- [23] Liaw DJ, Hsu PN, Chen WH, Lin SL. *Macromolecules* 2002;35:4669–76.
- [24] Li WM, Li SH, Zhang QY, Zhang SB. *Macromolecules* 2007;40:8205–11.
- [25] Cheng SH, Hsiao SH, Su TH, Liou GS. *Macromolecules* 2005;38:307–16.
- [26] Liou GS, Hsiao SH, Chen HW. *J Mater Chem* 2006;16:1831–42.
- [27] Wang HM, Hsiao SH. *Polymer* 2009;50:1692–9.
- [28] Hsiao SH, Liou GS, Kung YC, Pan HY, Kuo CH. *Eur Polym J* 2009;45:2234–48.
- [29] Kung YC, Hsiao SH. *J Mater Chem* 2011;21:1746–54.
- [30] Yen HJ, Liou GS. *Polym Chem* 2012;3:255–64.
- [31] Ling QD, Chang FC, Song Y, Zhu CX, Liaw DJ, Chan DSH, et al. *J Am Chem Soc* 2006;128:8732–3.
- [32] Kuorosawa T, Chueh CC, Liu CL, Higashihara T, Ueda M, Chen WC. *Macromolecules* 2010;43:1236–44.
- [33] Chen CJ, Yen HJ, Chen WC, Liou GS. *J Mater Chem* 2012;22:14085–93.
- [34] Yen HJ, Chen CJ, Liou GS. *Adv Funct Mater* 2013;23:5307–16.
- [35] Chen CJ, Yen HJ, Hu YC, Liou GS. *J Mater Chem C* 2013;1:7623–34.
- [36] Yu AD, Kuorosawa T, Ueda M, Chen WC. *J Polym Sci Part A: Polym Chem* 2014;52:139–47.
- [37] Seo ET, Nelson RF, Fritsch JM, Marcoux LS, Leedy DW, Adams RN. *J Am Chem Soc* 1966;88:3498–503.
- [38] Nelson RF, Adams RN. *J Am Chem Soc* 1968;90:3925–30.
- [39] Hagopian L, Kohler G, Walter RI. *J Phys Chem* 1967;71:2290–6.
- [40] Creason SC, Wheeler J, Nelson RF. *J Org Chem* 1972;37:4440–6.
- [41] Hsiao SH, Chang YM, Chen HW, Liou GS. *J Polym Sci Part A: Polym Chem* 2006;44:4579–92.
- [42] Kung YC, Liou GS, Hsiao SH. *J Polym Sci Part A: Polym Chem* 2009;47:1740–55.
- [43] Hsiao SH, Liou GS, Wang HM. *J Polym Sci Part A: Polym Chem* 2009;47:2330–43.
- [44] Liou GS, Chang CW. *Macromolecules* 2008;41:1667–74.
- [45] Ghaemy M, Alizadeh R, Behmadi H. *Eur Polym J* 2009;45:3108–15.
- [46] Zhang K, Niu HJ, Wang C, Bai XD, Lian YF, Wang W. *J Electroanal Chem* 2012;682:101–9.
- [47] Hsiao SH, Wang HM, Lin JW, Guo WJ, Kung YR, Leu CM, et al. *Mater Chem Phys* 2013;141:665–73.